

Article

# A Fast Calculation of Partially Corroded, Grounding-Resistive Electrode Electrical Parameters

**Gregorio Denche, Eduardo Faleiro \*, Gabriel Asensio  and Jorge Moreno**

Escuela Técnica Superior de Ingeniería y Diseño Industrial, Universidad Politécnica de Madrid, 20012 Madrid, Spain

\* Correspondence: eduardo.faleiro@upm.es

**Featured Application:** The proposed model can be applied to the assessment of the electrical parameters of non-perfect conducting grounding electrodes that are partially affected by corrosion.

**Abstract:** The calculation of the grounding resistance of electrodes built with partially oxidized non-perfect conductors is addressed in this paper. A model based on circuit analysis to account for internal resistance is used, while the oxidation or partial coating of the conductor surface is modeled using the concept of the equivalent radius of the coated electrode. From the proposed model, the values of the electrical parameters of the grounding electrodes, such as the grounding resistance and the step and touch potentials, are calculated for real electrodes affected by coating or corrosion and compared with those values under ideal conditions. The results show significant differences in certain configurations that may compromise the safety margins established by current regulations.

**Keywords:** non-perfect conducting grounding electrodes; coated electrode equivalent radius; partially corroded electrode



**Citation:** Denche, G.; Faleiro, E.; Asensio, G.; Moreno, J. A Fast Calculation of Partially Corroded, Grounding-Resistive Electrode Electrical Parameters. *Appl. Sci.* **2022**, *12*, 12243. <https://doi.org/10.3390/app122312243>

Academic Editors: Andreas Sumper and Roberto Zivieri

Received: 12 October 2022

Accepted: 25 November 2022

Published: 30 November 2022

**Publisher's Note:** MDPI stays neutral with regard to jurisdictional claims in published maps and institutional affiliations.



**Copyright:** © 2022 by the authors. Licensee MDPI, Basel, Switzerland. This article is an open access article distributed under the terms and conditions of the Creative Commons Attribution (CC BY) license (<https://creativecommons.org/licenses/by/4.0/>).

## 1. Introduction

Grounding systems are elements of an electrical installation of great importance for the protection of people and equipment [1]. When there is an electrical fault, the step and contact potentials must not exceed the values given in the current regulations, and the grounding resistance must be adjusted to the value of the potential acquired by the electrode in the case of a unitary fault current [2]. At the design stage, calculations are made taking into account several simplifying assumptions. Firstly, it is assumed that the conductors that are part of the grounding electrodes are perfect electrical conductors (PEC), that is, they do not have internal resistance. Second, the surface of these conductors is in intimate contact with the soil, so that it is treated as the interface between an ideal conducting medium, with no resistivity, and a conducting medium with a finite value of resistivity. Common additional assumptions are, for example, that the ground is semi-infinite and electrically homogeneous, the conductors that form part of the grounding electrode have a constant radius, or the fault current leaking to the ground does so at low frequency, called industrial frequency [3].

This paper embodies two substantial improvements to the most popular models to evaluate the electrical parameters of grounding electrodes, namely, the inclusion into the calculation of the internal resistance of conductors and the possible oxidation or coating of part of them. While the first does not present special difficulties to be taken into account in the well-known models, the second entails a formidable complication in the calculations unless some simple procedure makes it possible to evaluate the effect produced by the electrode coating.

The necessary modifications on an initial model based on the Charge Simulation Method (CSM) are presented in this paper. These modifications take into account both the internal resistance of the conductors [4] and their possible affection, in part or in its

entirety, by corrosion [5]. The oxidation is modeled as a layer of a conductive material with high resistivity that completely covers part of the conductors. Additionally, the new model can also evaluate the effect of coating conductors with a layer of any conductive material with arbitrary resistivity. If the conductors are considered as cylindrical rods, the oxidation or coating effect of these conductors is modeled by replacing their geometric radius by the so-called Coated Electrode Equivalent Radius (CEER) [6]. As a result of this substitution, an electrode composed of conductors with different geometric radius values according to their oxidation level or the nature of the coating is obtained. To take into account the internal resistance of the conductors, a circuit-based model (CBM) of the entire electrode, composed of branches and nodes, where the potential drops in the different branches due to the ohmic resistance are considered, gives rise to a complete description of the behavior of the electrode in terms of the currents flowing through the branches and those that leak into the ground [7]. According to the model proposed in this paper, the grounding resistance of the electrode is calculated as the ratio between the potential of the node in which the current is injected and the value of the injected current. The step and contact potentials on the ground surface are also evaluated by knowing the leakage currents to the ground [8]. Although the two basic elements of the paper, internal resistance and surface corrosion, have been previously modeled separately by the authors, the combination of both in a single model represents a new model that is broader than the previous two models. Aspects such as mixing different conductor radii into the structure due to electrode coating and combining clean conductor parts with other coated ones all embedded in multilayered soils represent a clear extension of the previous models.

In order to carry out all the tasks described above, after this introduction, this work presents a section with the fundamentals of the proposed model, followed by another section dedicated to applying the model to the calculation of the electrical parameters of some electrodes of interest. A single electrode and some actual electrodes currently in operation are considered. In all of them, the partial oxidation of some of the conductors that form part of the geometric structure of the electrodes has been simulated. In the same section, the electrical parameters calculated as ideal electrodes are compared with those obtained by applying the new model to the real electrode. The final section of the paper is dedicated to collecting the conclusions and final comments on the content of this work.

## 2. The Model Backgrounds

To calculate the electrical parameters of a grounding electrode, the simplest model assumes that the conductors are non-resistive PEC, so that the electrode as a whole is equipotential [9]. The incoming current through the injection point is distributed throughout the conductor and is filtered to ground through its surface so that the electrode becomes equipotential. The injection point is not important, and only the magnitude of the fault current is the initial relevant information. The leakage current to the ground in each part of the electrode is calculated without difficulty. With this information, the grounding resistance and potentials at the ground surface, with which step and touch potentials are evaluated, are calculated. Such potentials are important magnitudes since they characterize the electrical behavior of the electrode [10]. When the conductors that form part of the electrode have internal resistance, the electrode is no longer equipotential as a whole, and the injection point becomes important. The model that best describes the behavior of an electrode of this nature is the aforementioned CBM. According to this model, the electrode is divided into branches and nodes, and circuit theory is applied to each branch and each node. A complete description of the model can be found in the aforementioned reference [7], which describes the CBM of a buried electrode in a semi-infinite multilayer soil. The application of the model supplies the currents flowing through the branches and the leakage currents to the ground of each branch. With this information, the potential at any point on the ground can be calculated.

Figure 1 shows in the top a horizontal rod which is divided into N branches. The branch potential  $U_k$  and the leakage current  $I_k$  in each branch are also shown. At the bottom, the CBM

is shown. At each node of the circuit, the potential  $V_t$  and the source of nodal leakage current  $J_t$  are located. The internal currents  $i_k$  that run inside the conductor are also shown. Node potentials and branch potentials are closely related, as also are the nodal leakage currents and branch leakage currents. The branch potentials  $U_k$  depend on the currents filtered to the ground by all other branches  $I_m$ , including the branch  $k$  itself. Assuming that the electrode lies on the same soil layer with resistivity  $\rho$ , it can be stated that

$$U_k = \sum_{m=1}^N I_m \cdot Z_{km} \quad (1)$$

where the impedance  $Z_{km}$ , called transverse impedance, has the following expression for a multi-layered soil,

$$Z_{km} = \frac{\rho}{4\pi} \int_{l_m} dl_m \left[ \frac{1}{|\vec{r}_k - \vec{r}_m|} + \int_0^\infty (f(\lambda)e^{-\lambda(z_k - z_m)} + g(\lambda)e^{\lambda(z_k - z_m)}) J_0(\lambda r) d\lambda \right] \quad (2)$$

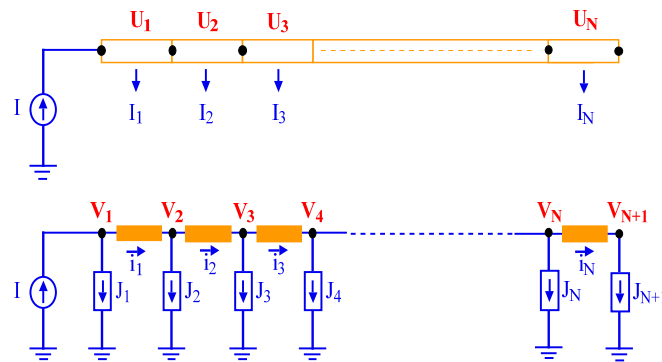


**Figure 1.** A picture of the circuit-based model of a rod buried into the soil.

As stated before,  $\rho$  is the soil resistivity around the branch  $m$ , and the functions  $f(\lambda)$  and  $g(\lambda)$  stand for the contribution of the other soil layers to the potential, which are calculated by imposing the boundary conditions at each layer interface [7]. The branch potentials  $U_k$  and the leakage currents  $I_m$  are then related with the node potentials  $V_k$  and currents  $J_m$ , which satisfy the CBM equations.

Next, the influence of a partial coverage of the electrodes will be introduced in the model. According to the results of the aforementioned reference [6], the presence of a layer that covers the surface of the conductors, either of oxide from the material of the electrodes or any other conductive material, modifies the potential associated with each branch, and the global effect is equivalent to the substitution of the initial radius of the conductors by a Coated Electrode Equivalent Radius (CEER) whose expression is, in the case of oxidation with an oxide layer of thickness  $e$ ,

$$r_{eq} = (r_C - e)^{\frac{\rho_{ox}}{\rho}} \cdot r_C^{-(\frac{\rho_{ox}}{\rho} - 1)} \quad (3)$$

while, for an electrode covered with a layer of material of thickness  $e$ ,

$$r_{eq} = r_C^{\frac{\rho_{co}}{\rho}} \cdot (r_C + e)^{-(\frac{\rho_{co}}{\rho} - 1)} \quad (4)$$

In both cases,  $r_C$  represents the radius of the conductor, not oxidized or not coated,  $\rho_{ox}$  is the resistivity of the oxide layer that covers the electrode,  $\rho_{co}$  is the resistivity of the coated layer, and  $\rho$  the resistivity of the soil, which is assumed to be semi-infinite and uniform [6]. Although Expressions (3) and (4) are valid for single-layer soils, they will also be used to modify the radius of the conductors, even in multilayered soils, provided that such conductors are completely embedded in any of the soil layers. It should be mentioned

that Expressions (3) and (4) represent a considerable simplification of the effect caused by the coating of the electrodes. The complex filtering mechanism of the current to the ground through the surface of the conductor and the interface that separates the covering layer from the ground is reduced to a geometric modification. A variable radius for the electrodes is relatively easy to implement in the calculation algorithms and does not significantly increase the computation time of the potentials.

To finish this section, it is necessary to mention that the proposed model has been implemented using the commercial software MatLab, which is especially suitable for carrying out the necessary calculations.

### 3. Application Examples

In all the application examples that will be presented, two types of calculation will be carried out in order to compare the results. The first type corresponds to the electrode considered as ideal or PEC. For this purpose, the general calculation method proposed in this paper will be used, assigning a very small internal resistivity. The second type of calculation considers electrodes with appreciable internal resistance. In practice, it is about comparing electrodes made with copper, which is the most used material and is considered to be an almost perfect conductor, with electrodes made of less conductive materials such as stainless steel, aluminum, or others. In the following examples, PEC or the ideal electrode stand for an electrode made of copper of resistivity  $\rho = 1.78 \times 10^{-8} \Omega\text{m}$ .

#### 3.1. Partially Oxidized Horizontal Rod

As a first example of application, consider a horizontal rod with length  $L = 40 \text{ m}$  and initial radius  $r_C = 5 \text{ mm}$ , buried 0.5 m from the surface of a uniform soil with resistivity  $\rho = 100 \Omega\text{m}$  and half covered with a layer of conductive material with resistivity  $\rho_{ox} = 500 \Omega\text{m}$  and thickness  $e = 1.5 \text{ mm}$ . The resistivity of the oxide layer and the thickness are fictitious in order to evaluate the effect on the electrical parameters of these added properties. The rod material has an internal resistivity  $\rho_e = 7 \times 10^{-6} \Omega\text{m}$ . The current injection point is at one of its ends, and the fault current is set at 1 A. The rod is segmented with 30 pieces per meter.

Figure 2 shows the Ground Potential Rise (GPR) produced by the resistive half-covered rod. A different profile is observed in the two halves. In order to compare the behavior of the ideal electrode with the real one, Figure 3 is included.

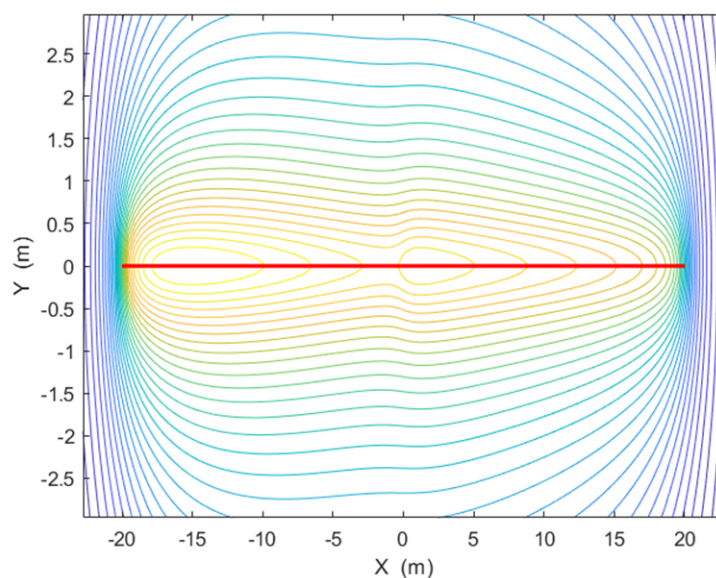


**Figure 2.** GPR contour plot from the partially oxidized horizontal rod the example 1.

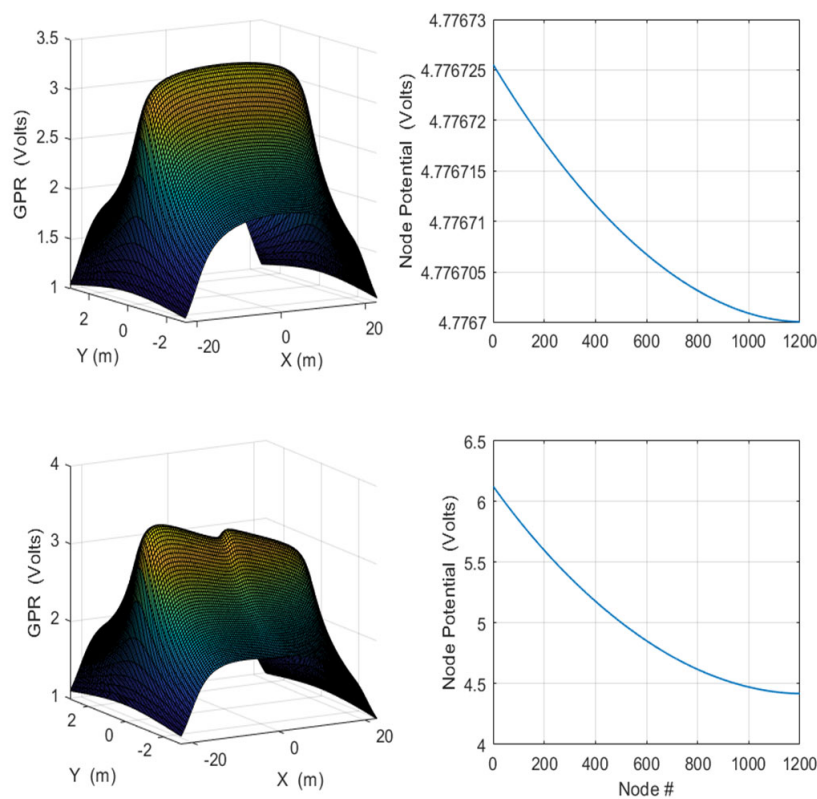


**Figure 3.** Some electrical features of the ideal horizontal rod (**upper** panels) and those of coated resistive horizontal rod (**lower** panels).

In the upper left panel of Figure 3, a surface plot of the GPR created by the ideal horizontal rod is shown. In the right panel, the potential at the nodes that join the 1200 segments into which the rod is divided is shown. The calculations have been made with copper as the internal resistivity, so it is really a PEC. It is observed that the potential can be considered constant along the length of the rod. In the lower panels, the results for the same rod, but considering both the finite internal resistance  $\rho_e$  and the influence of the covering layer of half its length, are shown. In this case, a strong potential gradient is observed along the conductor in addition to a potential profile on the surface that shows a clear difference between the two halves of the rod. In this simple example, given that the representative potential of the electrode is that associated with the injection node, it can be seen that there is a difference in grounding resistance between the two assumptions of more than 20%.

### 3.2. Grounding Grid of an Outdoor Transformation Center

As a second application example, the grounding grid of an outdoor transformation center, like the one shown in Figure 4, will be considered. Such a transformation center is a standard of some of the most important Spanish electrical companies, such as *Iberdrola* or *Endesa*. The soil is considered uniform with resistivity  $\rho = 100 \Omega\text{m}$ . The fault current will be set at 1 A, entering one of the corners. The material of the conductors has a resistivity  $\rho_e = 72 \times 10^{-8} \Omega\text{m}$  that corresponds to stainless steel [11]. For this case, it will be assumed that half of the electrode is oxidized (marked in black on Figure 5), forming a uniform layer of thickness  $e = 2 \text{ mm}$  of oxidized material, with a resistivity of  $\rho_{ox} = 800 \Omega\text{m}$ , throughout the length of the conductors affected by corrosion [12]. The segmentation is set to five pieces per meter. Although the resistivity of the oxide layer, and the thickness and length of the affected conductors do not correspond to any real situation, such data are taken from measurements made on similar conductors by the firm *INGESCO Lightning Solutions*, which is recognized in the acknowledgments.

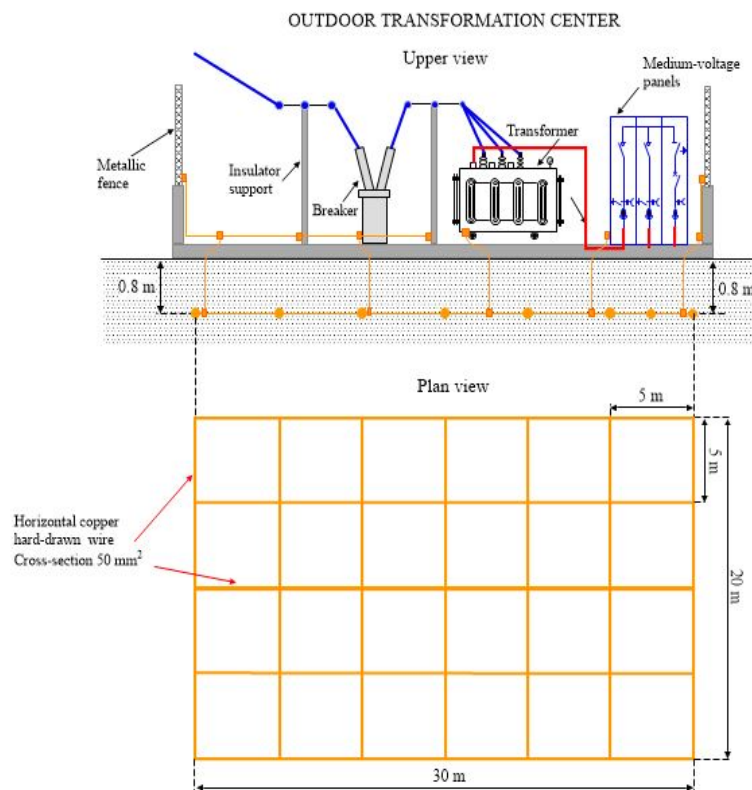


**Figure 4.** Example of grounding systems for an outdoor transformation center (Author source).

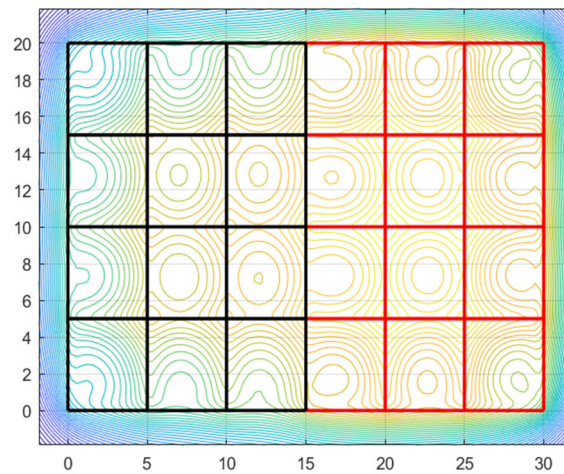


**Figure 5.** Ground Potential Rise contour plot from the grounding grid of the transformation center in Figure 4.

Figure 5 shows the GPR produced by the resistive half-covered grid. In this case, the internal resistivity is about forty times greater than that of copper, which is usually considered to be that associated with an ideal conductor.

In the upper left panel of Figure 6, the GPR of the PEC grid is shown. In the right panel, the node potentials of the ideal electrode are shown. The electrode is equipotential. In the lower panels, the same magnitudes are represented but considering the internal resistance  $\rho_e$  of the conductors and the partial oxidation of the electrode. It is shown that the potential profile in the ground is altered in the oxidized half of the electrode, while the potential of the nodes presents a clear, although small, gradient.

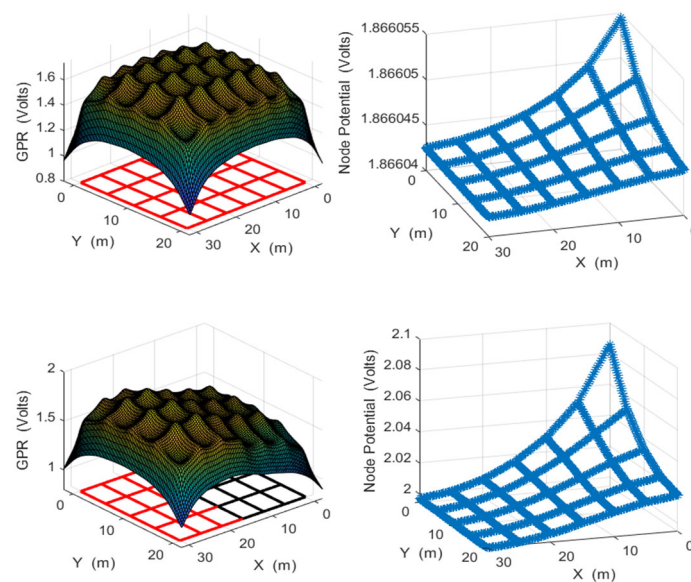


**Figure 6.** Some electrical features of the ideal grid (**upper panels**) and those of half-corroded resistive grid (**lower panels**).

To better appreciate the differences between considering the ideal electrode or including all the limitations, Figure 7 shows, on the left panel, the GPR percentage difference between the two situations, while on the right, the node potentials' percentage difference is shown. As seen in Figure 7, there is more than 10% difference in the potential of the current injection node between the ideal electrode and the real electrode, which also corresponds to the percentage difference in the grounding resistance of the mesh, since the fault current is unitary. Note that although the current input point is at a higher potential than the rest, the differences are not very close to 5%. However, these differences will increase as the electrode becomes larger. To conclude, it is necessary to point out that such a percentage difference may mean, in practice, being outside the regulations regarding installation safety.

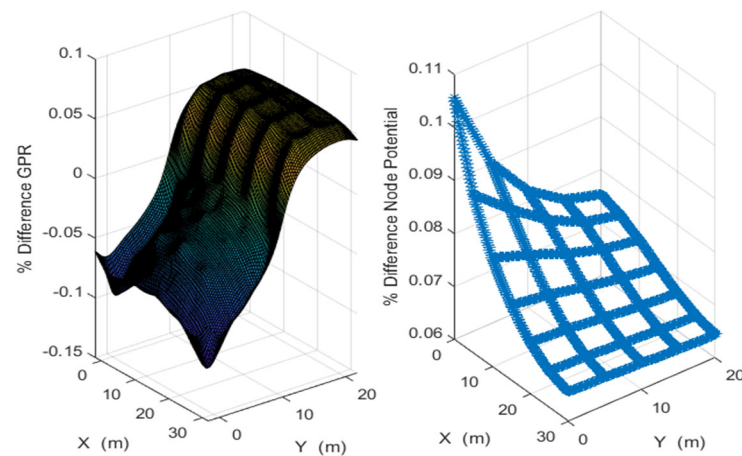


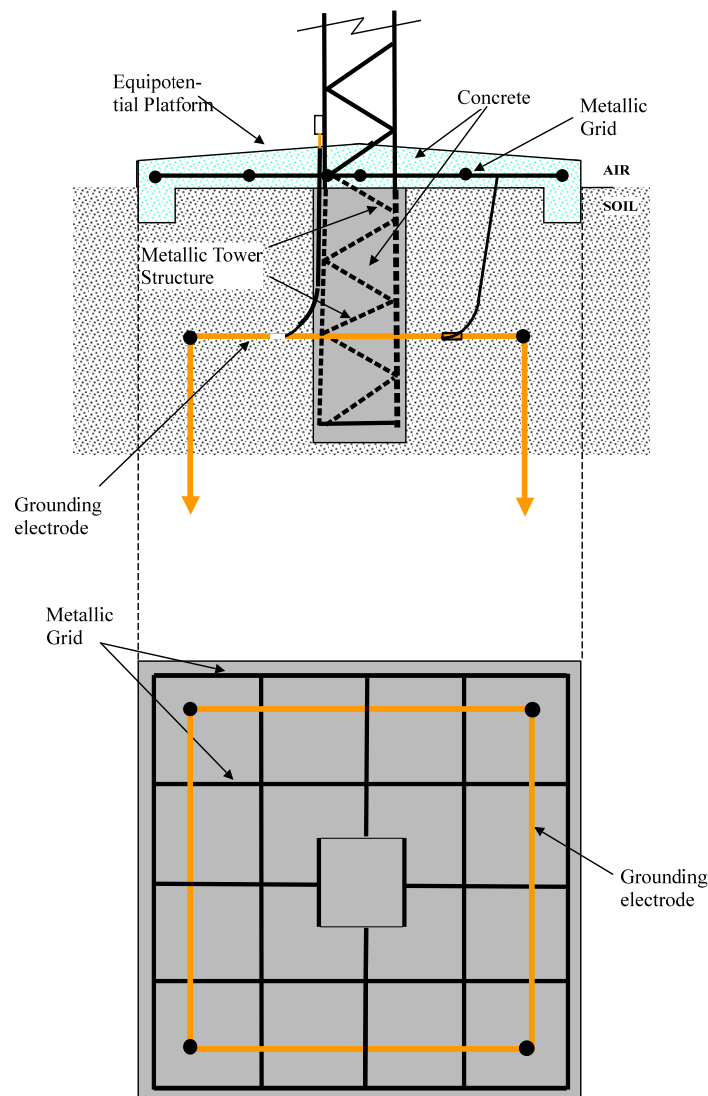
**Figure 7.** Percentage difference both in GPR and in the node potential when considering an ideal and a real grid.

### 3.3. Grounding Electrode Partially Coated with a High-Conductive Boost Material

In this third application example, a grounding electrode commonly used in transmission line towers will be considered. As in the previous example, this transmission line tower is a standard type of tower used by some of the most important Spanish electricity companies. In this example, the electrode is buried in a very high-resistivity soil  $\rho = 1000 \Omega\text{m}$ , so it is necessary to partially cover some of the conductors with a very low-resistivity material

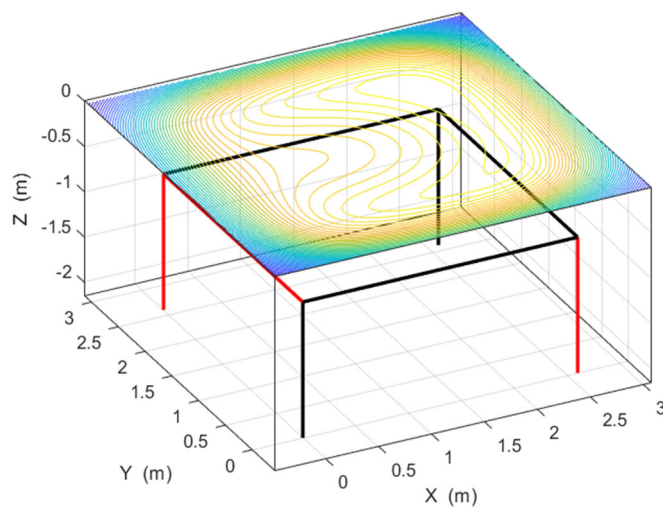
$\rho_{co} = 2.5 \Omega\text{m}$  to reduce the grounding resistance of the electrode. The material used for these coatings is bentonite, whose resistivity is between 2 and  $5 \Omega\text{m}$ , using thicknesses that vary according to the resistivity of the surrounding soil. In this case, it will be assumed that the material layer has a thickness of  $e = 2 \text{ cm}$ , and the conductors will have an internal resistivity of  $\rho_e = 72 \times 10^{-8} \Omega\text{m}$  corresponding to stainless steel.

Figure 8 shows the grounding electrode of a transmission line tower. It has a 2.6 m square frame and 1.5 m long vertical rods at the vertices, all buried at a depth of 0.65 m. The conductors have  $50 \text{ mm}^2$  cross sections.



**Figure 8.** Grounding system of a transmission line tower.

Assuming negligible the effect of the structure of the tower, including the surface platform, in the calculations, Figure 9 shows a contour plot of the GPR produced by the resistive, partially covered electrode. The covered parts of the electrode are marked in black. As in the previous examples, Figure 10 shows the differences between setting conductors as PEC (upper panels) without considering the coating of some of them and the real case in which both attributes are incorporated into the calculation of the grounding resistance and the potentials generated in the ground.



**Figure 9.** Ground Potential Rise contour plot from the grounding electrode of the transmission line tower in Figure 8.

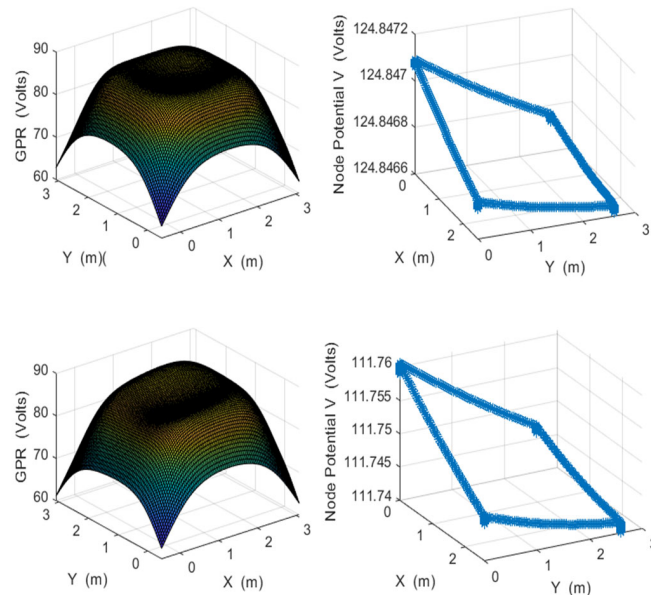


**Figure 10.** Some electrical features of the ideal electrode (**upper** panels) and those of the partially covered resistive electrode (**lower** panels).

For this configuration, a 10% reduction in grounding resistance can be achieved. Note that there are no significant differences in the potential of the nodes in the real electrode, mainly because the internal resistance is not very large and the electrode is relatively small in size. The percentage of reduction of the grounding resistance can be increased if the thickness of the layer of conductive material is increased.

### 3.4. Vertical Deep-Well Grounding Electrode Partially Corroded

From numerous measurements, it has been proven that the deep-well grounding technology has a smaller grounding resistance and a lower step voltage, while the area assigned to the installation is small and when in the lowest layer deep in the soil, where the vertical electrode is located, the resistivity is low [13]. In this example, a deep-well grounding electrode made of stainless steel rods with a 9 mm radius and 150 m long is driven into a fictitious horizontally three-layered soil with resistivities  $\rho_1 = 100 \Omega\text{m}$  thickness  $h_1 = 4 \text{ m}$ ,  $\rho_2 = 200 \Omega\text{m}$  thickness  $h_2 = 6 \text{ m}$ , and  $\rho_3 = 50 \Omega\text{m}$ . A part of the electrode located in the soil bottom layer, is covered with an oxide film of thickness  $e = 2 \text{ mm}$  and resistivity

$\rho_{ox} = 720 \Omega\text{m}$ . Once again, the oxide layer resistivity and thickness are fictitious for the purpose of assessing the effect on grounding resistance and other parameters. As already commented in Section 2, the CEER can still be applied if the oxidized part is entirely located in a soil layer. Due to the nature of the electrode, the potential at the ground surface will not present significant differences between the two electrode configurations considered, that is, as PEC and with real attributes. While it is to be expected that the grounding resistance will present appreciable differences, after dividing the rod into segments at a rate of three segments per meter, an electric current of 1 A is injected through its upper end, and the nodal potentials are calculated, especially the one associated with the input node of the current, in order to calculate the grounding resistance. The results of the application of the proposed model are summarized in Table 1.

**Table 1.** Grounding resistance of the deep-well electrode in different conditions.

	$\rho_e = 0 \Omega\text{m}$	PEC	$\rho_e = 72 \times 10^{-8} \Omega\text{m}$ (Non-Corroded)	$\rho_e = 72 \times 10^{-8} \Omega\text{m}$ ( $\rho_{ox} = 720 \Omega\text{m}$ )
<b>R(Ω)</b>	0.5567	0.5606	0.7063	0.7542
%	0	<1%	21.2%	26.2%

Table 1 clearly shows the influence of the two electrode conditions that are studied in this paper. The difference between completely ignoring the internal resistance of the electrode and taking the value of the resistivity of the copper instead impacts the grounding resistance by less than 1%. However, if copper is replaced by a material such as stainless steel, the difference rises to almost 21% if oxidation is not taken into account and up to 26% when including the effect of oxidation. As already mentioned in some of the previous examples, the effect of the internal resistance of the conductors intensifies with the size of the electrode. This example shows that the advantages of a long electrode driven into the ground are attenuated by the need to use materials other than copper with which to build the grounding electrodes.

#### 4. Conclusions

The commonly used model of the grounding electrode as a PEC without any signs of corrosion or alteration of the electrode surface has been improved in this work by including realistic attributes such as the internal resistance of the conductors and the possible damage caused by partial oxidation or by coating with a conductive material. In order to evaluate the impact of changes in the properties of the electrode, some important magnitudes have been calculated that define its characteristics, such as the GPR or the potential of the different nodes introduced in the modeling of the electrode. The grounding resistance is now associated with the potential of the fault current input node. In view of the results, it can be concluded that there is a significant difference between an ideal PEC electrode and an equivalent one with real attributes. For the example of the transformation center shown in Figure 2, the difference in grounding resistance is greater than 10%, and in terms of GPR, differences of around 5% are found. The differences increase with the extension and degree of oxidation of the electrode. In summary, the calculations obtained from the presented model confirm that the attributes included in the modeling of a real electrode, in particular the internal resistance, must be taken into account at the design stage to adjust the size and shape of the electrode in order to meet the safety requirements of current regulations.

Finally, although there may be many factors to consider that can affect ground resistance measurements, such as humidity, temperature, and other seasonal effects, oxidation is a systematic effect that can be detected in long-range measurements. The model presented in this paper would allow for an estimation of the degree of oxidation of an operational grounding electrode by comparing measurements of the real grounding resistance and its calculation using the model for a determined oxidation percentage, all without a high computational cost.

**Author Contributions:** Conceptualization, G.D. and E.F.; methodology, G.D., E.F. and G.A.; software, G.A. and J.M.; validation, G.D. and J.M.; formal analysis, G.D. and E.F.; investigation, G.D., E.F. and G.A.; data curation, J.M.; writing—original draft preparation, G.D. and E.F.; writing—review and editing, G.D., E.F., G.A. and J.M. All authors have read and agreed to the published version of the manuscript.

**Funding:** This research received no external funding.

**Acknowledgments:** The authors would like to thank the Department of Electrical Engineering, Applied Mathematics and Applied Physics of the Escuela Técnica Superior de Ingeniería y Diseño Industrial (ETSIDI) at Universidad Politécnica de Madrid (UPM) for their support to the undertaking of the research summarized here. Furthermore, the authors appreciate the collaboration with the firm INGESCO Lightning Solutions at Terrassa, Barcelona (Spain), for the technical support and data transfer from real cases studied in this work.

**Conflicts of Interest:** The authors declare no conflict of interest.

## References

1. IEEE Std 80TM-2013; (Revision of IEEE Std 80-2000/Incorporates IEEE Std 80-2013/Cor 1-2015). IEEE Guide for Safety in AC Substation Grounding. IEEE Power and Energy Society: Piscataway, NJ, USA, 2015; ISBN 978-0-7381-8850-8.
2. ENA, Energy Networks Association. *A Guide for Assessing the Rise of Earth Potential at Electrical Installations, Engineering Recommendation EREC S34, Issue 2*; Energy Networks Association: London, UK, 2017.
3. Ayodele, T.; Ogunjuyigbe, A.; Oyewole, O. Comparative assessment of the effect of earthing grid configurations on the earthing system using IEEE and Finite Element Methods. *Eng. Sci. Technol. Int. J.* **2018**, *21*, 970–983. [[CrossRef](#)]
4. Yuan, J.; Yang, H.; Zhang, L.; Cui, X.; Ma, X. Simulation of Substation Grounding Grids with Unequal-Potential. *IEEE Trans. Magn.* **2000**, *36*, 1468–1471.
5. Zhang, X.; Zhou, Z.; Chen, X.; Song, J.; Shi, M. Study on Corrosion Behavior of Copper-Clad Steel for Grounding Grids. In *Advances in Materials, Machinery, Electrical Engineering (AMMEE 2017)*; Atlantis Press: Amsterdam, The Netherlands, 2017; Volume 114.
6. Faleiro, E.; Asensio, G.; Denche, G.; Moreno, J. A fast method to compute the grounding resistance of a coated electrode using the coated electrode equivalent radius. *Electr. Power Energy Syst.* **2022**, *137*, 107879. [[CrossRef](#)]
7. Denche, G.; Faleiro, E.; Asensio, G.; Moreno, J. Grounding Electrodes with Internal Resistance: Application to Feasibility Study of the Driven-Rod Method for Modeling the Soil Electrical Resistivity Profile. *Appl. Sci.* **2021**, *11*, 5032. [[CrossRef](#)]
8. Moreno, J.; Pascual, P.; Faleiro, E.; Asensio, G.; Fernández, J.A. Estimation of an Upper Bound to the Value of the Step Potentials in Two-Layered Soils from Grounding Resistance Measurements. *Materials* **2020**, *13*, 290. [[CrossRef](#)] [[PubMed](#)]
9. Sunde, E.D. *Earth Conduction Effects in Transmission Systems*; Dover: New York, NY, USA, 1949. [[CrossRef](#)]
10. He, J.; Zhang, B.; Zeng, R. Maximum Limit of Allowable Ground Potential Rise of Substation Grounding System. *IEEE Trans. Ind. Appl.* **2015**, *51*, 5010–5016. [[CrossRef](#)]
11. Li, F.; Cui, Q. Research on the Properties of Copper-clad Steel in Substation Grounding Project. *Adv. Mater. Res.* **2012**, *354–355*, 1105–1110. [[CrossRef](#)]
12. Rajan, S.; Venugopalan, S.I. Corrosion and grounding systems. *IEEE Trans. Ind. Appl.* **1977**, *IA-13*, 297–306. [[CrossRef](#)]
13. Lu, H.; Jing, M.; C, H.; Hu, S.; Teng, Y.; Chen, J.; Lan, L.; Wen, X. Soil resistivity modeling for temperature rise calculating of HVDC deep-well earth electrode. *Electr. Power Energy Syst.* **2021**, *125*, 106537. [[CrossRef](#)]